



Cite this: *Dalton Trans.*, 2025, **54**, 11808

Received 15th July 2025,
Accepted 15th July 2025

DOI: 10.1039/d5dt01657f

rsc.li/dalton

A combined electrochemical and synthetic investigation was undertaken to probe aluminium's redox capabilities. Reduction from Al(III) to Al(I) occurs in a stepwise manner via Al(II). The highly reactive Al(I) species induces a catalytic electrochemical-chemical (EC) reaction, however, reversible redox processes are observed in the individual steps [Al(III) ↔ Al(II) and Al(II) ↔ Al(I)].

In the past ten years considerable progress has been made in low-oxidation state main group chemistry.^{1–3} In particular, low-oxidation state aluminium chemistry has flourished,^{4–7} from the isolation of the neutral dialumenes^{8–10} to exploiting Al(I) species in the activation of strong bonds *via* oxidative addition, such as those commonly found within waste emissions (*e.g.*, C–O, C–F).^{11,12} Furthermore, in 2018, the long-standing assumption that aluminium is always electrophilic was ended by an elegant method that exposed its latent nucleophilic character.¹³ Whilst these discoveries deepen our fundamental understanding of aluminium chemistry, synthetic challenges along with safety concerns due to the forcing conditions (*e.g.*, alkali metal reductions) often required to access low-oxidation state complexes, prevents the general uptake of low-oxidation state aluminium chemistry. For example, the first monomeric Al(I) complex was reported in 2000,¹⁴ and it has been shown to be a powerful tool for the main group chemist, from cleavage of strong H–X bonds to unique cooperative effects seen with heterobimetallic systems.^{15–20} However, the synthesis of this Al(I) (2) species is challenging (Scheme 1A) requiring vigorous stirring over potassium metal for three days followed by crystallisation to separate 2 from the mixture of products that are formed.¹⁴ As such its general use has largely been limited to a small section of the main group community despite its unique credentials.

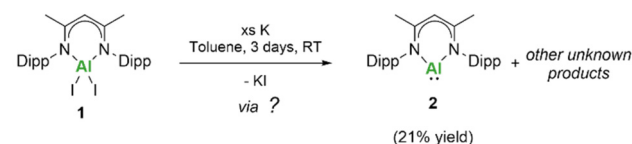
Probing the redox chemistry of β -diketiminate supported aluminium complexes†

Fáinché Murphy,[†] Madeleine Bell, Elyse Aitken, Brian G. McMillan* and Catherine E. Weetman^{†*}

Alternative routes to low-oxidation state aluminium complexes have focussed on the use of soluble and milder reducing agents such as Jones and Stasch's Mg(I) dimer and Roesky's Al(I) (2).^{21–24} These have resulted in a variety of Al(II) compounds which have been observed to undergo equilibrium processes. Notably, Nikonov reported the reaction of LiAlH_2 (L = β -diketiminate) with 2 which formally undergoes oxidative addition to yield the dimeric $[\text{LAlH}]_2$ species.²² The Al(II) complex reversibly undergoes disproportionation to Al(I) and Al(III) (Scheme 1B). Bakewell,²⁵ and Cowley²⁶ have further investigated this showing that the equilibrium processes can be exploited to access new Al(II) and Al(I) species through fine tuning of ligands and/or reaction conditions (Scheme 1C).

Whilst the above offer new synthetic strategies to access low-oxidation state aluminium complexes, the majority still

(A) Synthesis of Roesky's β -diketiminate Al(I)



(B) Equilibrium between Al(III) + Al(I) and Al(II)



(C) Reversible Reductive Elimination



Department of Pure and Applied Chemistry, University of Strathclyde, 295 Cathedral Street, Glasgow, G1 1XL, UK. E-mail: Brian.McMillan@strath.ac.uk, Catherine.Weetman@strath.ac.uk

† Electronic supplementary information (ESI) available: General synthetic experimental details, NMR spectra, electrochemistry. See DOI: <https://doi.org/10.1039/d5dt01657f>

Scheme 1 (A) Synthetic procedure for Roesky's Al(I) used in this study. (B) Observed equilibrium between β -diketiminate aluminium complexes. (C) Reversible reductive elimination processes for accessing new Al(II) and Al(I) species (Dashed and Dotted curved lines represent bidentate chelating ligands). Dipp = 2,6-diisopropylphenyl.



rely upon a trial-and-error approach with alkali metal based reducing agents to access new low-oxidation state main group compounds. This frequently results in over or under reduction, as well as large amounts of experimental waste. Given our interests in sustainability, we sought to circumvent the trial-and-error approach by establishing an electrochemical set up that was compatible with low-oxidation state main group complexes, particularly those of aluminium. This will provide the redox potentials, allowing for fine tuning of reducing agent, as well as keen insight into the fundamental electron transfer processes available to aluminium within defined complexes.

To start, we opted to study Roesky's β -diketiminate supported aluminium system (Scheme 1A)¹⁴ due to its prominence in the literature. Additionally, any insight into the mechanism of formation (*e.g.*, redox potentials) alongside the redox capabilities of the system will guide future discovery and may improve the synthetic efficiency of the reaction. Following initial trial-and-error with an electrochemical set-up (see ESI for details[†]), we found that a conventional three-electrode system consisting of a glassy carbon working electrode, a platinum counter electrode, and a silver pseudo-reference electrode, along with THF as the solvent and $[\text{NBu}_4][\text{PF}_6]$ as the electrolyte, provided an optimal set-up for our cyclic voltammetry (CV) experiments. Importantly, synthetic experiments showed that no reactivity was observed between compounds **1** or **2** with the solvent and/or electrolyte, within 1 hr at room temperature (*i.e.* conditions and time frame of the CV experiments).

Our initial CV of **1** revealed two irreversible reduction processes (Fig. 1A). These two distinct cathodic peaks demonstrate that two separate reduction processes occur in a stepwise manner. To study the nature of these reduction events, we varied the potential scan rate from 50 mV s^{-1} to 300 mV s^{-1} (Fig. 1B), with the peak currents for each increasing in a manner consistent with diffusion-controlled processes. Use of a ferrocene internal standard allowed for determination of the reduction potentials of **1**, and these were calculated as -2.34 V and $-3.23 \text{ V vs. Fc/Fc}^+$. The measured values are in line with those expected, considering the highly reducing conditions required to access Al(I) experimentally.

The CV of **1** indicates a likely catalytic electron transfer – chemical reaction mechanism (denoted EC') based on waveform shape and the large differences in current for the two reduction events.²⁷ The two step reduction process likely proceeds *via* an Al(II) species. Thus, to investigate the EC' mechanism we have used a combined synthetic and electrochemical approach. Firstly, to confirm the first reduction is a one electron transfer process we carried out Differential Pulse Voltammetry (DPV) and Squarewave voltammetry (SWV) using microelectrodes (Fig. 2). The full width at half maximum (FWHM) provided a value of 150 mV confirming a one electron transfer process for the first reduction peak, and the formation of an Al(II) species. Synthetically, reduction of **1** using 1.2 eq. 5% Na/NaCl or 1 eq. KC_8 in toluene led to the isolation of a new, pale-yellow complex (**3**) after 72 hrs at room temperature (Scheme 2). Compound **3** was characterised by multinuclear

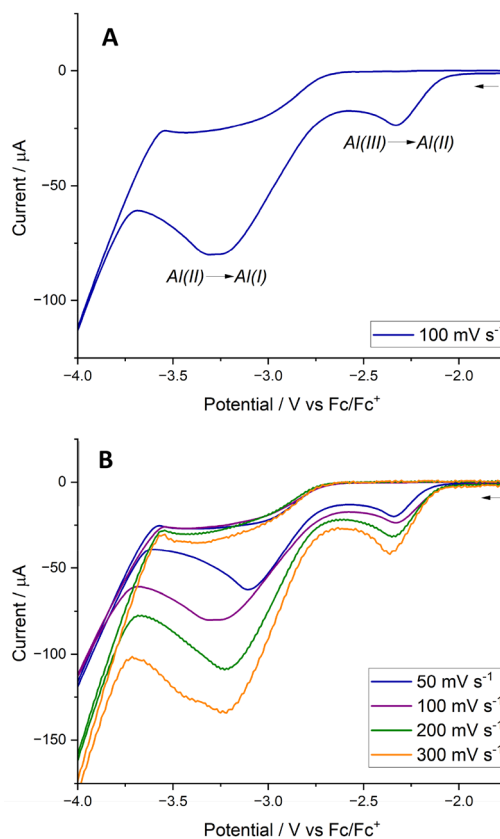


Fig. 1 (A) CV of **1** at 100 mV s^{-1} . (B) CV of **1** at varying scan rates.

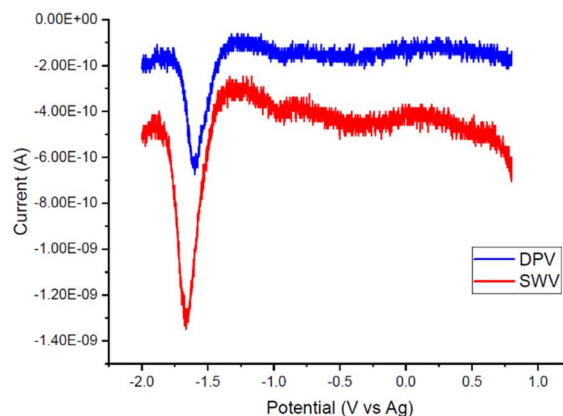
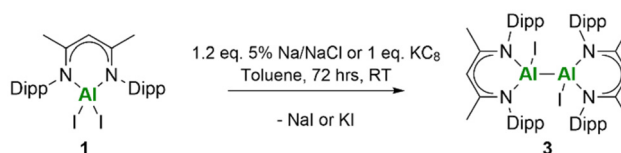


Fig. 2 DPV and SWV of the first reduction of **1**.



Scheme 2 Synthesis of Al(II) complex **3**.



and 2D NMR spectroscopy as well as elemental analysis and UV-vis spectroscopy. Unfortunately attempts at growing crystals suitable for single crystal X-ray crystallography was unsuccessful. The ^1H NMR spectrum of **3** is very similar to that of the starting material, with only a marginal shift in the β -diketiminato methine from $\delta 5.06$ ppm (**1**) to $\delta 5.07$ ppm (**3**). However, ^1H DOSY NMR reveals a clear difference in molecular weights with compound **3** almost double the estimated mass of **1** (see ESI for details[†]). Thus, we propose that **3** is the dimeric $[\text{LAlI}]_2$ Al(II) species, akin to the previously reported $[\text{LAlH}]_2$ dimer (Scheme 1B).²² As further proof that this species **3** is Al(II), we took the isolated compound **3** and reduced it with KC_8 . On monitoring the ^1H NMR spectra, 30% conversion to **2** was observed after 2 hrs, reaching a maximum of 39% conversion after 19 hrs then showed no further increase (Fig. S8[†]).

With a clearer understanding of the identity of the Al(II) species, we turned our attention back to the electrochemical investigation. Compound **1** exhibits irreversible reduction processes when scanning the whole potential window (*i.e.*, 0 V to -4.0 V *vs.* Fc/Fc^+), however, if only considering the first reduction window (*i.e.*, Al(III) to Al(II); -1.0 V to -2.6 V *vs.* Fc/Fc^+) reversibility can be achieved at higher scan rates (Fig. 3A). This supports the existence of a catalytic electrochemical –

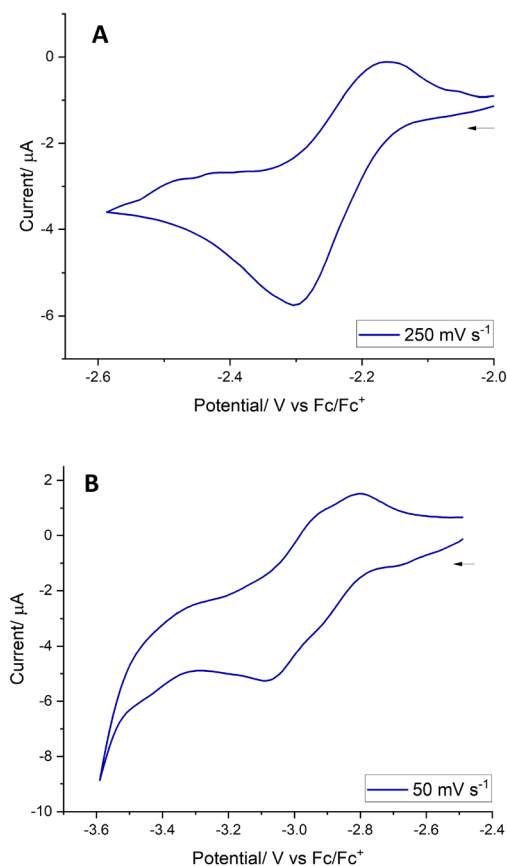
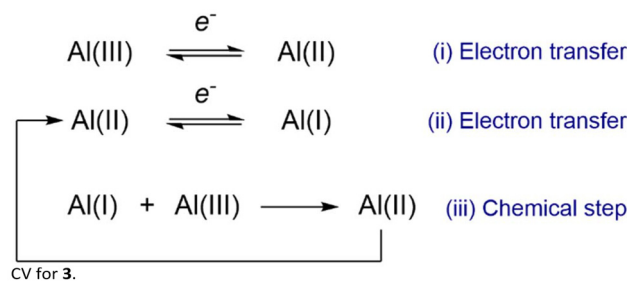


Fig. 3 (A) Al(III)–Al(II) reversible CV for compound **1**; (B) Al(II)–Al(I) reversible CV for **3**.

chemical reaction (EC') in this system. In an EC' reaction mechanism, the effect of chemical reaction depends on k/ν (rate of the chemical reaction/scan rate). If this ratio is large, the chemical reaction will have a significant effect on the reversibility of the system. Simply by increasing the scan rate, it is possible to force the electrochemical reaction to occur at a faster rate than the chemical reaction, allowing a level of reversibility to be observed.

Since we could synthetically isolate the Al(II) complex **3**, we were able to use it as a starting point within the electrochemical investigations to examine the Al(II) to Al(I) process. Keeping the potential window between -2.5 V to -3.6 V *vs.* Fc/Fc^+ , resulted in the observation of a reversible redox process at lower scan rates (50 mV s^{-1}) (Fig. 3B). Notably, this reduction also occurs at a higher potential -3.08 V *vs.* Fc/Fc^+ (**3**) than for compound **1** (-3.23 V *vs.* Fc/Fc^+). This difference of 150 mV in the reduction potentials indicates a different chemical composition of **1** and **3**. This is expected, as electrochemical reduction reactions involve the addition of an electron whilst the chemical reduction involves the cleavage of an aluminium–iodide bond.

Based on electrochemical data, we postulate that the irreversible behaviour observed in the full electrochemical window (starting from **1**, Fig. 1A) is therefore the result of the chemical reaction between **1** [Al(III)] and **2** [Al(I)] to yield **3** [Al(II)] (Scheme 3iii). Reversibility is only observed in the system in the individual electron transfer steps (Scheme 3i and ii) as shown in Fig. 3. This is in line with the proposed EC' reduction mechanism and matches the observed equilibrium reaction for the corresponding hydride system reported by Nikonov (Scheme 1B). To test this experimentally, we turned to NMR investigations. Combining **1** with **2** in d_8 -toluene did not result in an observed reaction at room temperature or elevated temperatures (50 $^\circ\text{C}$). However, changing the reaction solvent to d_8 -THF in line with electrochemical experiments results in the formation of **3**, indicating oxidative addition of **1** to the Al(I) centre of **2** (see ESI for details[†]). Importantly here, we do not observe the disproportionation reaction of **3** back to **1** and **2** (*i.e.* a chemical reaction and no observed equilibria). This contrasts with the previously reported equilibrium for the corresponding hydride system by Nikonov and co-workers.²²



Scheme 3 Mechanistic interplay between Al(III), Al(II), and Al(I) complexes, from electrochemical observations.



In conclusion, we have been able to establish an electrochemical set-up that is compatible with low-oxidation state main group species and determine the redox potentials of Roesky's β -diketiminato aluminium system. Electrochemical investigations revealed a catalytic electrochemical-chemical (EC) reduction mechanism, in which the stepwise reduction processes were found to be reversible but in the presence of Al(III) starting material (from the bulk solution) the electrochemically generated Al(I) species will chemically react in an irreversible manner. Exploration of the electrochemical properties of other low-oxidation state main group systems is ongoing, with a view to developing redox-based catalytic cycles at main group centres.

Author contributions

FM performed the synthetic and electrochemical experiments, MB performed the initial electrochemical investigation and EA performed the microelectrode study. BMcM and CEW conceptualised the study, supervised the project, and finalised the manuscript for submission.

Conflicts of interest

There are no conflicts to declare.

Data availability

Data that supports the findings of this study are available from the University of Strathclyde Knowledge Base Pure data repository at <https://doi.org/10.15129/e19896e1-4b1e-41a6-93e9-0d0abef3bc60>.

Acknowledgements

We thank Craig Irving for assistance with NMR spectroscopy, Beatriz Doñagueda Suso for elemental analysis, and the Mulvey, O'Hara, Robertson groups for many insightful discussions. This work was supported by the Royal Society Research Grant RG\R1\251254. CEW would like to thank the University of Strathclyde for the award of a Chancellor's Fellowship and the award of a PhD studentship (FM).

References

- 1 P. P. Power, *Nature*, 2010, **463**, 171–177.
- 2 C. Weetman and S. Inoue, *ChemCatChem*, 2018, **10**, 4213–4228.
- 3 R. L. Melen, *Science*, 2019, **363**, 479–484.
- 4 C. Weetman, H. Xu and S. Inoue, Recent Developments in Low-Valent Aluminum Chemistry, in *Encyclopedia of Inorganic and Bioinorganic Chemistry*, 2024.
- 5 K. Hobson, C. J. Carmalt and C. Bakewell, *Chem. Sci.*, 2020, **11**, 6942–6956.
- 6 J. Hicks, P. Vasko, J. M. Goicoechea and S. Aldridge, *Angew. Chem., Int. Ed.*, 2021, **60**, 1702–1713.
- 7 M. P. Coles and M. J. Evans, *Chem. Commun.*, 2023, **59**, 503–519.
- 8 P. Bag, A. Porzelt, P. J. Altmann and S. Inoue, *J. Am. Chem. Soc.*, 2017, **139**, 14384–14387.
- 9 C. Weetman, A. Porzelt, P. Bag, F. Hanusch and S. Inoue, *Chem. Sci.*, 2020, **11**, 4817–4827.
- 10 R. L. Falconer, K. M. Byrne, G. S. Nichol, T. Krämer and M. J. Cowley, *Angew. Chem., Int. Ed.*, 2021, **60**, 24702–24708.
- 11 T. Chu and G. I. Nikonov, *Chem. Rev.*, 2018, **118**, 3608–3680.
- 12 M. R. Crimmin, M. J. Butler and A. J. P. White, *Chem. Commun.*, 2015, **51**, 15994–15996.
- 13 J. Hicks, P. Vasko, J. M. Goicoechea and S. Aldridge, *Nature*, 2018, **557**, 92–95.
- 14 C. Cui, H. W. Roesky, H.-G. Schmidt, M. Noltemeyer, H. Hao and F. Cimpoesu, *Angew. Chem., Int. Ed.*, 2000, **39**, 4274–4276.
- 15 M. Zhong, S. Sinhababu and H. W. Roesky, *Dalton Trans.*, 2020, **49**, 1351–1364.
- 16 Y. Liu, J. Li, X. Ma, Z. Yang and H. W. Roesky, *Coord. Chem. Rev.*, 2018, **374**, 387–415.
- 17 F. Rekhroukh, W. Chen, R. K. Brown, A. J. P. White and M. R. Crimmin, *Chem. Sci.*, 2020, **11**, 7842–7849.
- 18 R. Y. Kong and M. R. Crimmin, *Dalton Trans.*, 2021, **50**, 7810–7817.
- 19 M. Batuecas, N. Gorgas and M. R. Crimmin, *Chem. Sci.*, 2021, **12**, 1993–2000.
- 20 N. Gorgas, A. J. P. White and M. R. Crimmin, *J. Am. Chem. Soc.*, 2022, **144**, 8770–8777.
- 21 S. J. Bonyhady, D. Collis, G. Frenking, N. Holzmann, C. Jones and A. Stasch, *Nat. Chem.*, 2010, **2**, 865–869.
- 22 T. Chu, I. Korobkov and G. I. Nikonov, *J. Am. Chem. Soc.*, 2014, **136**, 9195–9202.
- 23 X. Wang, R. F. Ligorio, F. Rüttger, D. M. J. Kregel, N. Graw, R. Herbst-Irmer, A. Krawczuk and D. Stalke, *Dalton Trans.*, 2024, **53**, 15441–15450.
- 24 F. Murphy, A. R. Kennedy and C. E. Weetman, *Dalton Trans.*, 2025, **54**, 6038–6042.
- 25 C. Bakewell, K. Hobson and C. J. Carmalt, *Angew. Chem., Int. Ed.*, 2022, **61**, e202205901.
- 26 R. L. Falconer, G. S. Nichol, I. V. Smolyar, S. L. Cockcroft and M. J. Cowley, *Angew. Chem., Int. Ed.*, 2021, **60**, 2047–2052.
- 27 C. Sandford, M. A. Edwards, K. J. Klunder, D. P. Hickey, M. Li, K. Barman, M. S. Sigman, H. S. White and S. D. Minter, *Chem. Sci.*, 2019, **10**, 6404–6422.

